Journal of Marine Systems 79 (2010) 134–143

Contents lists available at ScienceDirect

Journal of Marine Systems

journal homepage: www.elsevier.com/locate/jmarsys

Identification, characteristics and seasonal evolution of surface thermal fronts in the Argentinean Continental Shelf

Andrés L. Rivas *, Juan Pablo Pisoni

Centro Nacional Patagónico (CENPAT-CONICET), Boulevard Brown s/n, (9120) Puerto Madryn, Chubut, Argentina

A R T I C L E I N F O

Article history:
Received 27 January 2009
Received in revised form 13 May 2009
Accepted 22 July 2009
Available online 6 August 2009

Keywords:
Surface thermal fronts
Argentinean Continental Shelf
Satellite SST data

A B S T R A C T

The location and seasonal variability of surface thermal fronts along the Argentinean Continental Shelf (38–55°S) were studied using 18 years (1985–2002) of sea surface temperature (SST) satellite data. Monthly SST gradients were calculated and a threshold was used to identify frontal pixels. Frontal areas were classified into 4 zones according to their seasonal evolution and the main forcings leading to the front's formation were identified for each group. The shelf break front was easily detected due to the large number of frontal pixels in the region and its high mean gradient values. This front showed a marked annual cycle and relatively constant position associated to the bottom slope; it tended to be located where the core of the Malvinas current is closest to the shelf. Tidal fronts also showed a strong annual cycle, being detected in three well-defined regions during spring and summer. Along the coasts of Tierra del Fuego and Santa Cruz, the combination of strong tidal mixing and low-salinity coastal plumes led to semi-annual seasonal cycles of frontal intensity and persistence that showed a relative maximum in winter. A similar behavior (semi-annual) was found at the coast off the Buenos Aires Province. There, the coastal dilution and the bathymetric gradient generated near-coastal fronts that changed direction seasonally. In the northern mid-shelf, a front linked to the intrusion of warm waters formed in the San Matías Gulf was identified during the winter.

1. Introduction

An oceanic front is a region in the ocean where abrupt changes of any hydrographic property are produced, i.e. an area where the horizontal gradient of this property reaches high values. Normally, these regions are narrow zones that separate wide areas with different vertical structure (stratification) and/or different water masses. Despite the relatively small area occupied, fronts and water circulation related to them are of importance since they regulate salt and heat transport, sea–atmosphere interactions, and the ecosystem.

For the Argentinean Continental Shelf (ACS), Bianchi et al. (2005) used horizontal salinity distribution to identify four water masses delimitated by the presence of different fronts of diverse origins. These fronts are clearly distinguishable from surface temperature gradients (see Fig. 3b in Palma et al., 2004 and Fig. 2a in Bogazzi et al., 2005), at least in the warm period (October–March in the Southern Hemisphere). Acha et al. (2004) studied the frontal regions detected near the southern end of South America, along the Atlantic and Pacific coasts, and their relation with several ecological processes documented in the region. These authors mentioned the occurrence of estuarine fronts which, at first, would not show a signal in the temperature field and thus would not be detectable in the SST satellite data. Sabatini et al. (2004) also mentioned the presence of haline fronts near 51°S and their influence on zooplankton distribution. Saraceno et al. (2004) analyzed surface thermal fronts in the Southwestern Atlantic Ocean from 9 years of NOAA–AVHRR data (1987–1995). These authors focused their study on the oceanic and the shelf break regions to define frontal areas and to analyze their intensity and persistence.

Identification of persistent fronts and the quantification of the seasonal cycle in the occurrence of SST fronts from satellite data offer a large-scale perspective that is impossible to obtain with *in situ* observations. In addition, a series of almost 20 years of systematic data is currently available to analyze long term variability in a region that has been historically undersampled. Surface thermal gradients detected in areas where the surface heat flux is almost uniform, are generated where horizontal advection (horizontal heat flux) and/or stratification (i.e. vertical heat flux) suddenly change. Neither of these processes can be successfully analyzed only with surface (satellite) data. However, in the ACS the available *in situ* information is scarce and scattered, being the satellite information as a powerful tool to describe the evolution, intensity and size of frontal areas.

Notwithstanding the significance of fronts in regulating both physical and biological processes taking place at the ACS (Bianchi et al., 2005; Romero et al., 2006; Rivas et al., 2006; Rivas, 2006; Bianchi et al., 2009), a reliable inventory of SST fronts is still absent. While the annual evolution of some fronts is almost unknown, other fronts are known to be seasonal but there are almost no literature references

* Corresponding author. Fax: +54 2965 451543.
E-mail address: andres@cenpat.edu.ar (A.L. Rivas).

0924-7963/$ – see front matter © 2009 Elsevier B.V. All rights reserved.
doi:10.1016/j.jmarsys.2009.07.008

about the months when they develop or reach their maximum magnitude. References indicating orientation and magnitude of such fronts are almost nonexistent. The purpose of this work is to use 18 years of AVHRR data to identify persistent and large-scale frontal structures present in the ACS, south of 38°S, and study the seasonal variability in their intensity, persistence and extent from the climatological point of view. The association of fronts with bottom topography and their relation to oceanographic and atmospheric variables are discussed and compared with previously available information.

This paper has been organized as follows: after this introduction, in Section 2 we present the data, methods and the zones used for the analysis. In Section 3 we show the results. Finally, summary and conclusions are given in Section 4.

2. Data and methods

2.1. Data

Eighteen years of SST data (from January 1985 to December 2002) obtained by the Advanced Very High Resolution Radiometer (AVHRR) on board NOAA satellites, processed by the Pathfinder project version 4.1, available at http://poet.jpl.nasa.gov, were used for this study. These data consist of 216 monthly composite images with a resolution of about 9 km, which cover the area in the Southwestern Atlantic defined by parallels 38 and 55°S, the 1000 m isobath and the coast.

2.2. Front detection

The detection of fronts from SST data can be performed using different procedures (see for example Shimada et al., 2005; Belkin and O´Reilly, 2009), but two basic methodologies are commonly used. One, developed by Cayula and Cornillon (1992), identifies the presence of a front when the temperature histogram is bimodal in a local window. The second one estimates the horizontal gradient of the temperature field, and uses a threshold to distinguish a front from background values. Ullman and Cornillon (2000) evaluated the performance of both methodologies and concluded that local histogram-based methods are more efficient in avoiding the detection of false fronts though they are more prone to miss real fronts.

In this work, fronts were detected using horizontal gradients of the SST field because it is a simple and effective method to detect edges in digital images and is widely used in a variety of applications (Belkin and O´Reilly, 2009). SST derivatives were computed using a centered difference scheme in both directions, zonal and meridional. The monthly gradient vector (hereon MGV) value was calculated for each grid point. SST values were analyzed in the proximities of those pixels where the gradient magnitude was higher than 0.5 °C km^{-1}, ruling out those considered contaminated by clouds presence. The threshold was estimated using the technique described by Saraceno et al. (2004), given that this criterion avoids the detection of spurious fronts. The cumulative frequencies of MGV magnitudes (normalized by the maximum value for such month) were estimated with a resolution of 0.005 °C km^{-1}. The cumulative histogram of MGV magnitudes for each month showed two different pixel categories; one, with low MGV magnitudes (background or frontless pixels) and one with large ones (frontal pixels). There was a high percentage of pixels under the first category and a small percentage under the second one. The threshold to separate both categories was defined as the MGV magnitude in the cumulative frequency plot that minimized the distance to the extreme (0 °C km^{-1}, 100%) (see Fig. 1). For each of the 216 months of data we determined when or not each pixel was frontal by comparing the gradient value with the threshold estimated for each month.

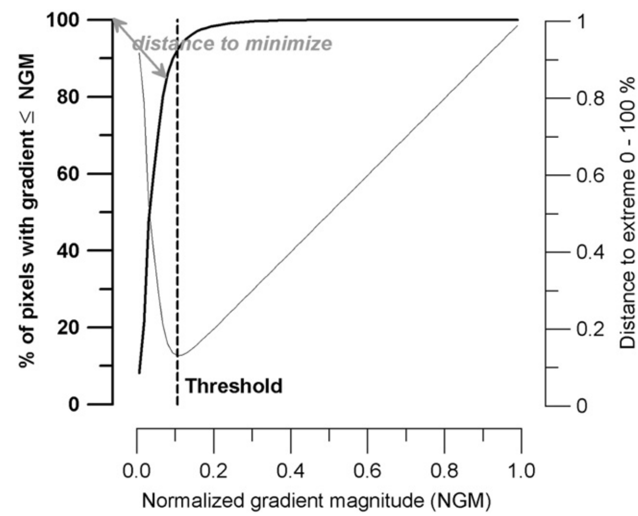

Fig. 1. Cumulative histogram (heavy line, left axis) of the normalized gradient magnitudes and distance (thin line, right axis) between the cumulative histogram curve and the point (0, 100%). The threshold was determined by finding the normalized gradient magnitude that minimizes the distance to the extreme (0, 100%).

We calculated for each calendar month, using only those pixels with more than 80% of valid data (15 over 18 or more), the following statistics:

a. the probability of detecting a front at a particular pixel, by dividing the number of times the pixel was frontal by the number of valid data for that month (i.e. frequency of occurrence),
b. the 12 climatological mean of MGV magnitude (CMGVm) and the components of the SST derivative (zonal and meridional),
c. the 12 climatological mean direction of the MGV (CMGVd), using the mean SST derivative components, and
d. the 12 climatological mean threshold using the 216 monthly threshold gradients. From the climatological point of view, a pixel was considered as frontal in a month if the CMGVm was greater than the climatological threshold.

After these calculations, for each pixel with more than 80% of valid data, we obtained the monthly climatological mean gradient magnitude (CMGVm) and direction (CMGVd), the knowledge of whether or not a pixel was climatologically frontal, and the probability that each pixel was frontal in a given month.

2.3. Seasonal evolution

In order to interpret the seasonal evolution of the fronts and to relate it to the possible causal mechanisms, we decided to restrict the analysis to those pixels found to be climatologically frontal for at least two of the 12 months, and to split the study area into different zones. We define a zone as the group of these frontal pixels inside the areas shown en Fig. 2 and identified four zones based on the analysis of the next statistics:

- mean CMGVm, averaged over all the zone constituent pixels. This variable gives an idea of the spatial heterogeneity of the SST field in the zone.
- mean CMGVm, averaged only over the zone constituent pixels that were frontal in the month under consideration. This variable gives an idea of the contrast in SST at both sides of the front for that month.
- the normalized size of the frontal area or the probability of finding a frontal pixel in the zone under consideration, calculated as the number of frontal pixels in a certain month divided by the total number of pixels that constitute the zone.

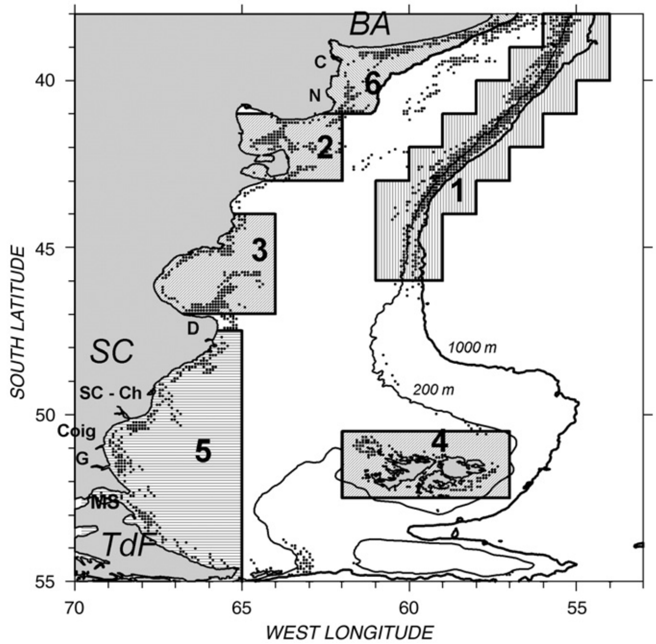

Fig. 2. Argentinean Continental Shelf (ACS) region. The solid lines are the 200 m and 1000 m isobaths. Map delineating the areas referred in the text: (1) shelf break zone, (2, 3 and 4) tidal zone, (5) Santa Cruz coastal zone and (6) Buenos Aires coastal zone. Black dots indicate pixels that were climatologically frontal for at least two out of the 12 months. Abbreviations are BA, Buenos Aires province; SC, Santa Cruz province; TdF, Tierra del Fuego province; C, Colorado river; N, Negro river; D, Deseado river; SC–Ch, Santa Cruz–Chico rivers; Coig, Coig river; G, Gallegos river and MS, Magellan Strait.

- the mean probability of detecting a front in a month, calculated only over the zone constituent pixels that were frontal in the month under consideration. This variable shows the persistence of the frontal pixels. For example, if a pixel was frontal during a certain month only for a given year, but its gradient value was high enough to force the climatological mean to be above the climatological threshold, the pixel was considered as climatologically frontal. Despite a pixel could be considered as frontal based on a unique extremely high gradient value, the frontal probability would remain very low.

The four zones considered (Fig. 2) are: shelf break zone (area 1), tidal zone (areas 2, 3 and 4), Santa Cruz coastal zone (area 5) and Buenos Aires coastal zone (area 6). This zonation included most of the two month climatologically frontal pixels. In Section 3.5 we make a reference to some frontal pixels not included inside these zones.

3. Results

The CMGVm showed that the location, size and intensity of the frontal zones change along the year (Fig. 3). Different color scales were used for each graph and those pixels where the gradient magnitude was higher than the estimated climatological threshold for each month were indicated in yellow and red colors. This allows to visualize clearly the shifts in position and size that frontal zones present every month. The CMGVm fluctuates throughout the year. While in September CMGVm is below 0.086 °C km^{-1} in all the pixels, in May some pixels show a CMGVm higher than 0.163 °C km^{-1}. Even when these extreme values found in particular pixels are not representative of “the intensity” of a frontal zone, they show that the magnitude of the discontinuity of the SST field varies among zones and from month to month. The seasonal evolution of the monthly front detection probability showed that those pixels with a detection probability higher than 0.5 (light blue line in Fig. 3) were almost exactly the same as those identified as frontal (yellow and red pixels in Fig. 3). For those pixels where MGV magnitude is higher than the threshold in more than half of the years (probability higher than 0.5) it is reasonable to expect that the CMGVm exceeds the climatological threshold. The agreement among frontal and high detection probability pixels indicates that fronts are both temporal and spatially persistent.

Belkin et al. (2009) report the first global remote sensing survey of thermal fronts in the Large Marine Ecosystems (LME) and, in our area of interest their results agree partially with ours. Although in the south zone there are remarkable differences between the fronts identified in this work and those described by Belkin et al. (2009), both works agree in the identification of the fronts North of 42°S that are not found in the literature. Regularly spaced, nonphysical zonal banding of high CMGVm (see for example between 50 and 51°S in Fig. 3, January) and, to a lesser extent, front detection probability (not shown) were observed. This banding is the result of small but detectable jumps in the Pathfinder SST values at regular intervals (18 pixels ≈ 163 km) in the meridional direction, arising as an artifact of the data interpolation to the equal-angle Pathfinder grid (see http://www.nodc.noaa.gov/sog/pathfinder4km/userguide.html and Ullman et al., 2007). We used the data as provided because meridional jumps are negligible for most of our purposes. Our analysis included only the study of the mean properties of the pixels identified as frontal. In Fig. 3 it can also be seen that some pixels with gradient values relatively high tend to align in trajectories that seem to follow the bathymetric contours.

3.1. Shelf break zone

The shelf break front is one of the most cited in the literature, probably because of its biological relevance. In this zone, two water masses meet: cold waters vertically mixed and under the influence of strong horizontal advection (Malvinas Current) and typical shelf waters, less vertically mixed and thus more sensitive to seasonal changes in surface heat fluxes. During the Austral spring–summer period, heat transferred from the atmosphere is more efficiently used by shelf waters to increase their SST than by the Malvinas Current waters where the horizontal advection and the vertical mixture are more intense. During the cold period, surface cooling produces vertical convection over the shelf and SST homogenization over the region. As a result, a larger amount of frontal pixels with high gradient magnitudes and frontal probabilities were observed along the October–May period than between June and September (Fig. 4). The surface location and extension of the frontal zone were in good agreement with the results obtained by Bogazzi et al. (2005) based on *in situ* data. Using the same satellite data as in the present work, Franco et al. (2008) found a complex structure for this front between 39 and 44°S, reflected in gradient magnitude variations perpendicular to the bathymetry. These authors considered this structure as a result of possible multiple branches of the Malvinas Current. Saraceno et al. (2004) and Franco et al. (2008) analyzed some aspects of the seasonal variability and they also found an annual cycle that reaches its greatest development in summer.

3.2. Tidal zone

The ACS is known as a region where tidal energy dissipation reaches very high values (Egbert and Ray, 2001 and references

Fig. 3. Mean monthly SST gradient magnitude averaged over the 1985–2002 period (CMGVm). The black lines are the 200 m and 1000 m isobaths. Note that the scale is different for each plot. Climatologically frontal pixels are indicated in yellow and red tones. The light blue line is the 0.5 monthly front detection probability contour.

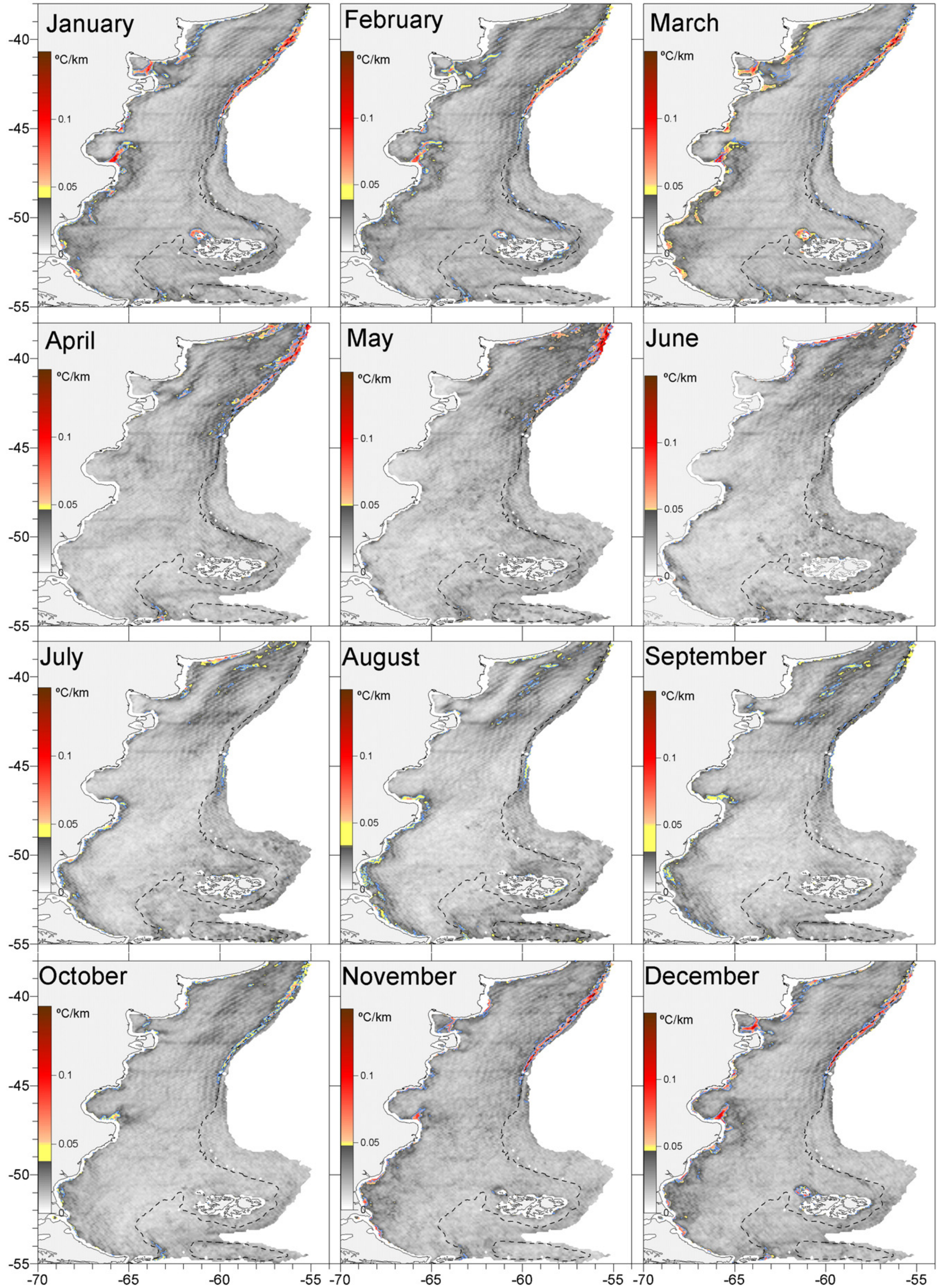
January
February
March
April
May
June
July
August
September
October
November
December
ºC/km
0.1
0.05
0
-40
-45
-50
-55
-70
-65
-60
-55

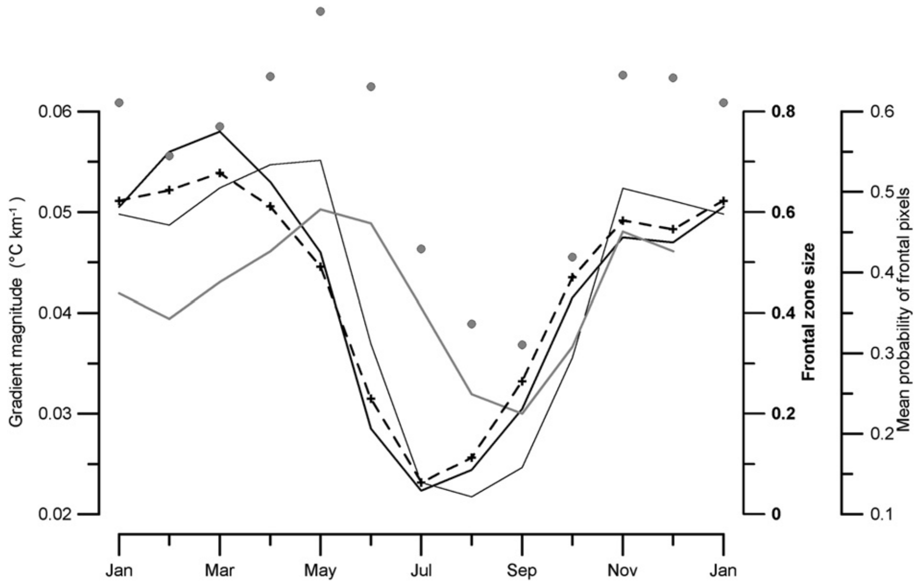

Fig. 4. Seasonal cycle in the shelf break zone. Mean monthly front detection probability averaged only over the zone constituent pixels that were frontal in the month under consideration (heavy dashed line and crosses); mean CMGVm averaged over all the zone constituent pixels (thin line); normalized size of the frontal area or the probability of finding a frontal pixel in the zone under consideration (heavy line); mean CMGVm averaged only over the zone constituent pixels that were frontal in the month under consideration (gray points) and climatological thresholds (gray line).

therein). High tidal energy dissipation zones have been located using different numerical simulations (Glorioso and Flather, 1995; Palma et al., 2004) without much discrepancy. In these zones, mixing caused by tidal currents generates enough turbulence to keep the water column homogeneous even during the warm period, and to give rise to different tidal fronts at the offshore edge of highly turbulent regions. These tidal fronts (three frontal areas, see Fig. 2 for identification) have been included in the tidal zone. During spring and summer they separate a relatively cool, shallow, vertically homogeneous zone, from warm (at the surface), stratified and deeper waters. These fronts weakened from March–April when the sea starts to cool down from the surface (and becomes vertically homogeneous) and reappeared in October, when the heat flux from the atmosphere to the sea returns (Fig. 5). Glorioso (1987), Glorioso and Simpson (1994), Sánchez et al. (1998) and Sabatini and Martos (2002), among others, have described this type of fronts (summarized in Bogazzi et al., 2005).

Shelf break and tidal fronts showed a similar seasonal variation since both originate at the limit between a vertically mixed zone and a zone that stratifies during the heat gaining period. Whereas the shelf break front persists until autumn (May), tidal fronts vanish as soon as the heat loss at the surface begins. Such difference can be understood by taking into account that the strong horizontal advection of cold water related to the Malvinas Current intensifies the cooling in the oceanic zone and retains the thermal gradient with the shelf zone, even after it has started to transfer heat to the atmosphere. Likewise, although to a lesser extent, strong vertical mixing and horizontal advection by the Malvinas Current delay surface heating and facilitates the establishment of the SST front during the heat gaining period. Consequently, it can be inferred that the shelf break front is associated with the differences in vertical mixing and horizontal advection presents between shelf and ocean waters.

These two kinds of fronts were also different in the direction of their SST gradient. During spring and summer, when the shelf break front was wider and more intense, the highest SST values were on the shelf, where the water column was shallower and stratified. On the other hand, tidal fronts were preferentially over shoal zones, which present appreciable depth changes and in different directions, which make the relation between SST and depth gradients not very clear. However, we speculated that during the heat gaining period tidal fronts were generated when the SST in the shallower zone was lower than in the stratified, deeper zone. In order to show this difference we calculated the p factor defined by Ullman and Cornillon (2001) as the normalized scalar product:

$$p = \frac{\nabla T.\nabla H}{|\nabla T|.|\nabla H|}$$

where T is the temperature and H is the water depth ($H<0$). The value of p ranges from -1 to 1 with the minimum (maximum) value corresponding to the case of cold (warm) water on the shallow side of a front positioned parallel to the isobaths. A value of zero indicates a front positioned perpendicular to the local isobaths.

The direction of the SST gradients (and in consequence the p parameter) was estimated only for those pixels of the zone that were frontal in the month under consideration.

Afterwards, the number of warm (highest SST in the shallowest region: $0.6<p\leq 1$) and cold fronts (highest SST in the deepest region: $-0.6>p\geq -1$) was registered at each zone for each month. During the spring–summer season, warm fronts prevailed at the Shelf Break zone (Fig. 6a) while in the tidal zone cold fronts were predominant (Fig. 6b).

3.3. Santa Cruz coastal zone

Using numerical simulations Glorioso and Flather (1995) and Palma et al. (2004) identified areas along the coasts of Santa Cruz and Tierra del Fuego provinces (South of 47.5°S), where tidal energy dissipation is quite important (area 5 in Fig. 2). These areas presented high values of monthly mean gradient magnitude (Fig. 3) and frontal probability. However, the seasonal variation in these frontal areas was not the one expected for a tidal front that vanishes during the cold season (when sea loses heat to the atmosphere).

The frontal zone located in the coastal region off Tierra del Fuego and Santa Cruz, was identified by Acha et al. (2004) as the Atlantic Patagonia cold estuarine front and described as a plume of diluted water, vertically mixed by tides and winds. It can be traced up to the 100 m isobath in the offshore direction and northward to the

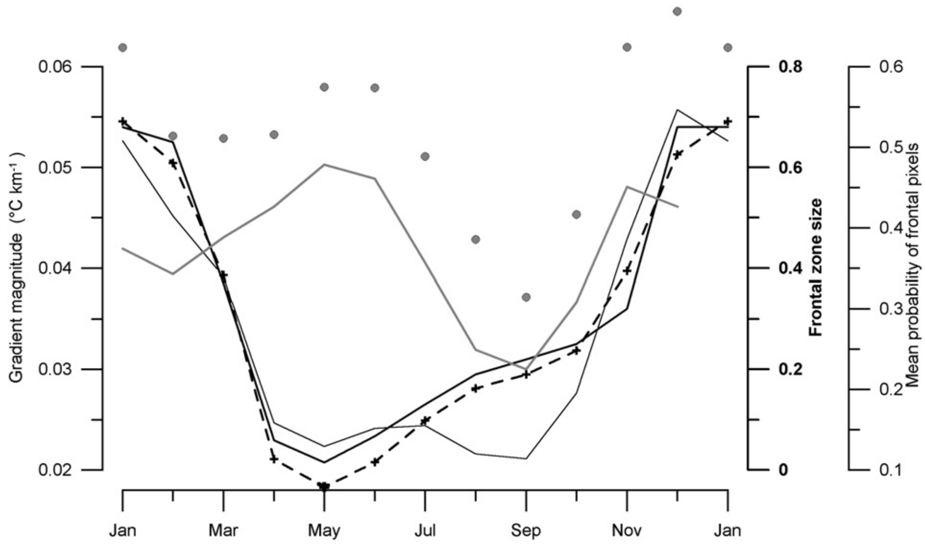

Fig. 5. Idem Fig. 5 but for the tidal zone.

southern end of the San Jorge Gulf. The seasonal evolution of this front (Fig. 7) showed a semi-annual cycle with maximum values in winter (July–August) and summer (December), though the number of frontal pixels, gradient magnitude and frontal probability were still high during spring (September and October). The formation of surface temperature fronts in this zone depends not only on the tidal mixing and the stabilizing effect of the surface heat flux but also on the discharge of continental waters (Gallegos, Coig, Santa Cruz, Chico and Deseado rivers, see Fig. 2 for location and for information over mean discharge and typical hydrographs of these rivers, see Pasquini and Depetris, 2007) and on the very low-salinity water coming from the Magellan Strait. Santa Cruz river, the most important of these rivers, reaches mean maximum discharge values of 1300 $m^3 s^{-1}$, while the contribution of diluted water that enters from the Magellan Strait is not known. However, historical hydrographic data from the shelf (Figure 1 in Guerrero and Piola, 1997) indicate that surface water salinity at the frontal zone is lower ($S<33.0$) than in the surrounding waters. In addition, Sabatini et al. (2004) found a weak vertical stratification at the inshore side of the fronts during the summer season (their Fig. 8) suggesting that fronts may represent the offshore edge of a freshened coastal zone.

In Fig. 7 we also show the monthly mean gradient magnitude calculated using just frontal pixels and it can be seen that in winter fronts were, in average, less intense than in summer. So the contrast between SST values at both sides of the fronts was slighter in winter, although the number of frontal pixels was higher. The temperature signal in this group appeared to be the result of summer warming and winter cooling of a near shore trapped band of low-salinity water as it

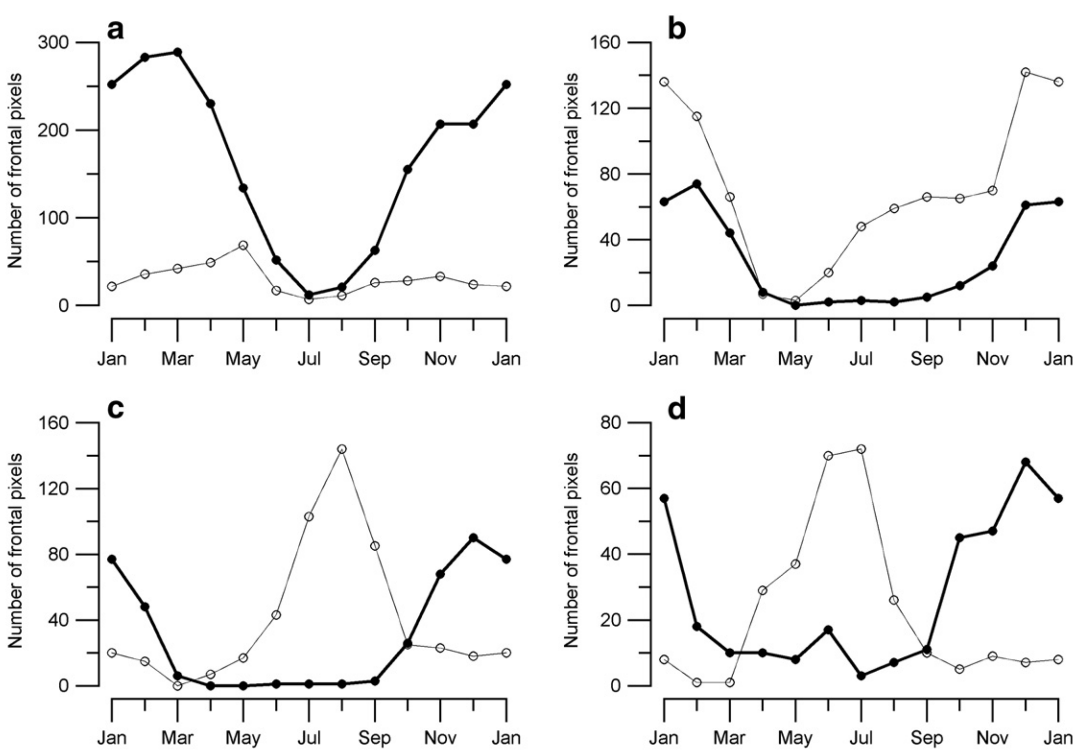

Fig. 6. Seasonal cycle of the mean monthly number of warm (heavy line) and cold (thin line) frontal pixels over the 1985–2002 period, for the shelf break zone (a), the tidal zone (b), the Santa Cruz coastal zone (c) and the Buenos Aires coastal zone (d).

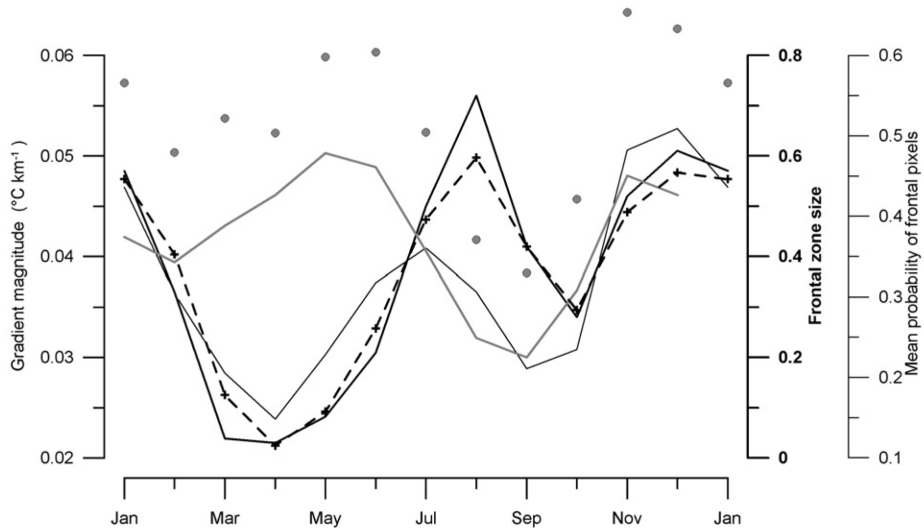

Fig. 7. Idem Fig. 5 but for the Santa Cruz coastal zone.

can be inferred from the evolution of the monthly mean gradient direction. The gradient directions (Fig. 6c) showed a marked seasonal variability. During the months of heat gaining by the ocean there were observed more warm fronts, indicative of warmer SST on the inshore (shallow) side. The few cold fronts detected during spring and summer could be originated in pixels where tidal mixing is intense enough as to overcome the stratification generated by the dilution caused by continental water discharges.

Ullman and Cornillon (2001), using a simple model, explained the evolution of the water cooling in a shelf with diluted water discharge. They simulated the formation of these types of fronts in winter and concluded that temperature acts as a tracer of salinity changes. In concordance with our results (Fig. 7), they showed that in winter the temperature gradient at the surface is weak.

3.4. Buenos Aires coastal zone

This zone is limited by parallels 38 and 41°S, the coast and the 50 m isobath. This area is very shallow, vertically mixed by tides (Lucas et al., 2005) and under the influence of the Negro and Colorado rivers (maximum volume transport of 1200 and 280 $m^3 s^{-1}$ respectively, for more information over mean discharge and typical hydrographs of these rivers, see Pasquini and Depetris, 2007). Its seasonal evolution (Fig. 8) showed a well-defined semi-annual cycle with few frontal pixels of low intensity and persistence by the end of summer (March) and early spring (September), while showed high values in June and December.

As we mentioned before, a similarity in temporal variation exists between the shelf break and tidal fronts. Now we found that the seasonal evolution of Santa Cruz and Buenos Aires coastal fronts also

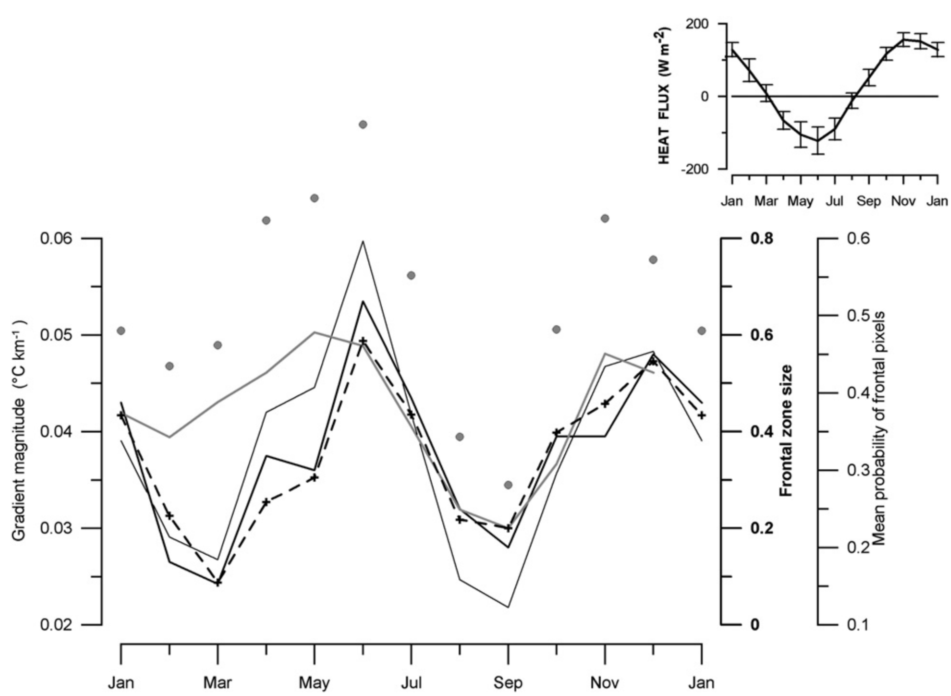

Fig. 8. Idem Fig. 5 but for the Buenos Aires coastal zone. The monthly mean climatological values and standard deviations of surface heat flux derived from NCEP reanalysis (Kalnay et al., 1996) estimated over the 1985–2002 period at 39.05°S, 60°W, are shown in the inserted graph.

showed certain similarities. In this case they share the same type of driving mechanisms: fresh water supply and tidal mixing.

In the Northern coastal region of this zone (less exposed to continental discharges), data reported by Lucas et al. (2005), showed that the mean temperature of the water column was higher in shallow waters during spring and summer and in deeper waters during autumn and winter. These authors estimated the Simpson stability parameter and found that, even during the warm season, the water column was vertically mixed; consequently, we can infer that SST and mean temperature of the water column are equal throughout the year. If the water column remains mixed, the thermal inertia offered by this column to the surface heat flux is proportional to the total depth. During the warm period, when the ocean gains heat, temperature at the coastal zone (shallow) did not differ significantly from the surface temperature found offshore (deeper waters) where there was some stratification and the heat flux down to the bottom was limited. As a consequence, summer gradients were weaker. In winter, with the same energy loss, shallower coastal waters become cooler.

The freshwater discharge gives rise to a thinner coastal superficial layer which is consequently more exposed to atmospheric fluxes, generating an effect similar to that caused by the bathymetric gradient. However, in the more diluted zones (the shallow sub-zone near the mouths of Negro and Colorado rivers) maximum SST gradient intensities were registered in summer, while winter fronts were weaker, since dilution competes with superficial cooling. Both bathymetric and dilution effects are present in this zone, generating fronts of high intensity both in winter (June) and summer (November) (Fig. 8). On the contrary, in the coastal region of Santa Cruz (Fig. 7) where coastal dilution is a preponderant factor, as we mentioned before, winter (July–August) fronts were less intense than in summer (December).

Frontal pixels identified in this zone are probably also influenced by Northern advection of San Matías Gulf waters particularly in winter (see Fig. 9).

Seasonal evolution of frontal statistics in this zone (Fig. 8) can be interpreted considering the variability of the surface heat flux (insert in Fig. 8 shows the climatological mean of net heat flux from the NCEP node located at 39.05°S–60°W, Kalnay et al., 1996). The majority of frontal pixels, with the highest probability and intensity, were observed in June, when surface heat loss to the atmosphere was highest. A secondary maximum occurred in November, when heat gain was at its maximum, and the front virtually vanished in March and August–September, when surface heat flux was lower.

Estimated CMGVd showed a marked seasonal variability (Fig. 6d). During the months of heat gain the gradient vector pointed towards the shallow area (where warm fronts prevailed) and during the months of heat loss, the gradient vector orientation was basically offshore (predominance of cold fronts indicates that SST grows towards deeper zones). Seasonal changes in SST gradient direction were consistent with the presence of a surface layer, exposed to the atmospheric heat flux, that gets thinner towards the coast, due to either continental dilution or bathymetric effects.

3.5. Pixels outside the four considered zones

We found a group of pixels classified as climatologically frontal for at least two months (Fig. 2) in the central zone of the shelf, between 38 and 43°S. Those pixels were identified as frontal only during winter, from June to September (Fig. 3), being absent between November and February. The presence of these frontal pixels could be associated with the outflow of water from San Matías Gulf. The warmer water tongue advected northerly from the San Matías Gulf was observed between July and September (Fig. 9). Frontal pixels were located in the southeastern end of this tongue, more exposed to the advection of cold water from the platform. Palma et al. (2008), using a numerical simulation of the Southwestern Atlantic shelf region circulation, reproduced the intrusion during winter of San Matías Gulf water (saltier and warmer) into the central shelf. These authors considered the presence of this mass of warmer and saltier water as the result of the development of a counterclockwise gyre at El Rincón Bight, which generates a stagnant zone which facilitates the intrusion of the San Matías Gulf waters. Belkin et al. (2009) also found a front over this zone but failed to mention its seasonality.

4. Summary and conclusions

Frontal regions located along the ACS were identified using a statistical description of their seasonal evolution. The use of an 18-year data series, the great spatial stability of the fronts and the use of space–time averaged parameters, give robustness to the present analysis.

Monthly mean distributions of CMGVm and probability (Fig. 3) showed the tendency of frontal pixels with high gradient magnitude and high probability of being frontal to gather in small, well-defined areas, which indicates that fronts are spatial and temporally persistent. This persistence allowed us to arrange most of the pixels considered as frontal, in four zones, each one having a distinct

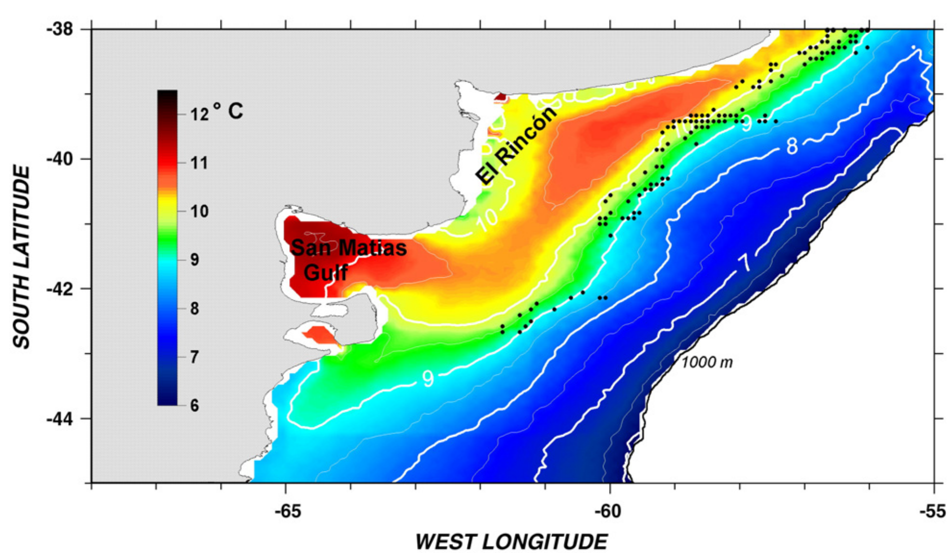

Fig. 9. Mean SST averaged over 1985–2002 for winter (July–September). Black dots indicate pixels that were climatologically frontal for at least one of the months considered.

seasonal evolution, which helped to infer the mechanisms involved in the generation of the fronts.

The whole region under study consisted of 17196 pixels (after ruling out those contaminated by the presence of clouds), 1600 of which showed a climatologic frontal behavior for at least two months. So it can be estimated that less than 10% of the region is associated to frontal zones.

The location of these zones is strongly conditioned by the bathymetry, which explains the great spatial stability of the fronts. Frontal pixels that characterize the transition from shelf waters to Malvinas Current waters are distributed along those shelf break zones where the bathymetric gradient is more intense, allowing the core of the current to stay near the shelf waters. Almost no frontal pixels were found along the shelf break south of 45°S where 200 and 1000 m isobaths separate and the bathymetric gradient softens. This result disagrees with Belkin et al. (2009). The location of the tidal fronts is determined by the presence of head-lands and shoals, which intensify the vertical mixing. Fronts found along Santa Cruz coast are located in the coastal zone, influenced by continental discharge. And finally, fronts located along the coast of Buenos Aires province have their origin where coastal dilution and bathymetric gradients allow differential heating/cooling of coastal and shelf waters, in a zone not deeper than 50 m.

Temporal variation of SST gradient magnitudes and monthly mean directions, relative size of frontal areas and the probability of the front's occurrence in each of the four zones (Figs. 4–8) allowed us to analyze their seasonal evolution and its association with the possible driving mechanisms. The seasonal variability showed distinctive characteristics in each of the four zones, presumably related to peculiarities in the local forcings (such as topography, tides, coastal dilution or heat flux).

Sometimes the behavior observed in a zone does not exactly coincide with what would be expected according to the identified forcing. One reason for this could be that not all the pixels of that zone respond to the same driving forces. As the analysis of the seasonal behavior of each zone is performed based on mean spatial values, if the number of pixels considered is large enough and its selection is appropriate, the method used here allows to identify the most robust and significant characteristics of the annual cycle. For example, in the tidal zone, which includes the tidal fronts, a few frontal pixels (those where gradient intensity is above the threshold value) can be observed even in winter when the entire area should be vertically mixed. In this case it is very likely for some pixels to be affected by coastal dilution, thus contaminating the predominant behavior of the area.

The present study allowed the identification of the frontal systems located at the ACS and to associate its different surface manifestations to diverse frontogenic mechanisms. The formation of a front is the result of concurrent driving forces. The dominant frontogenic mechanisms were discussed in each one of the four cases analyzed in this paper.

In the coasts of Tierra del Fuego and Santa Cruz the identified fronts show a semi-annual cycle (Figs. 3 and 7) while their orientation changes from summer to winter (Fig. 6c). This behavior is associated to the influx of cold and relatively fresh water through the Magellan Strait (see Palma et al., 2008 for numerically estimated Magellan outflow) and, to a lesser extent, to river discharges. The mixture by tides is intense all along the south coast (until ~40°S) but it becomes the main mechanism North of 47°S, where the effects of the continental discharge are weaker. A series of frontal pixels associated to the dissipation by tides described in different numerical simulations (Glorioso and Flather, 1995; Palma et al., 2004) was also identified around the Falklands Islands during spring and summer. Near El Rincon, a frontal zone with, again, a semi-annual behavior is originated by the decreased tidal amplitude together with an increase in the continental discharge associated with zonal bathymetric particularities. This interpretation, together with that for the Santa Cruz coastal zone, is strengthened by the changes in the orientations shown in Fig. 6d. The shelf break front is a transition zone between subantarctic shelf waters and the cold, salty and relatively nutrient-rich waters of the Malvinas Current. It is associated with a band of high superficial chlorophyll (Saraceno et al., 2005; Romero et al., 2006; Rivas et al., 2006) attributed to different upwelling mechanisms (Saraceno et al., 2005; Matano and Palma, 2008).

Acknowledgments

SST data were obtained from NASA Physical Oceanography Distributed Active Archive Centre at the Jet Propulsion Laboratory. We acknowledge S. Romero and R. Amoroso for their critical comments on the manuscript and also thank N. Glembocki for language corrections. This research was partially supported by Fundación Antorchas grant N° 13900-13 and PIP N° 112 20080103105 project.

References

Acha, E.M., Mianzan, H.W., Guerrero, R.A., Favero, M., Bava, J., 2004. Marine fronts at the continental shelves of austral South America. Physical and ecological processes. Journal of Marine Systems 44 (1–2), 83–105.

Belkin, I.M., O´Reilly, J.E., 2009. An algorithm for oceanic front detection in chlorophyll and SST satellite imagery. Journal of Marine Systems 78, 319–326.

Belkin, I.M., Cornillon, P.C., Sherman, K., 2009. Fronts in large marine ecosystems. Progress in Oceanography 81 (1–4), 223–236.

Bianchi, A.A., Bianucci, L., Piola, A.R., Ruiz Pino, D., Schloss, I., Poisson, A., Balestrini, C.F., 2005. Vertical stratification and air–sea CO2 fluxes in the Patagonian shelf. Journal of Geophysical Research 110, C07003. doi:10.1029/2004JC002488, 2005.

Bianchi, A.A., Ruiz Pino, D., Isbert Perlender, H.G., Osiroff, A.P., Segura, V., Lutz, V., Luz Clara, M., Balestrini, C.F., Piola, A.R., 2009. Annual balance and seasonal variability of sea-air CO2 fluxes in the Patagonia Sea: their relationship with fronts and chlorophyll distribution. Journal of Geophysical Research 114, C03018. doi:10.1029/2008JC004854.

Bogazzi, E., Baldoni, A., Rivas, A.L., Martos, P., Reta, R., Orensanz, J.M., Lasta, M., Dell'Arciprete, P., Werner, F., 2005. Spatial correspondence between areas of concentration of Patagonian scallop (*Zygochlamys patagonica*) and frontal systems in the Southwestern Atlantic. Fisheries Oceanography 14 (3), 1–18.

Cayula, J.F., Cornillon, P.C., 1992. Edge detection algorithm for SST images. Journal of Atmospheric and Oceanic Technology 9, 67–80.

Egbert, G.D., Ray, R.D., 2001. Estimates of the M_2 tidal energy dissipation from TOPEX/Poseideon altimeter data. Journal of Geophysical Research 106 (C10), 22475–22502.

Franco, B.C., Piola, A.R., Rivas, A.L., Baldoni, A., Pisoni, J.P., 2008. Multiple thermal fronts near the Patagonian shelf break. Geophysical Research Letters 35, L02607. doi:10.1029/2007gl032066.

Glorioso, P.D., 1987. Temperature distribution related to shelf-sea fronts on the Patagonian Shelf. Continental Shelf Research 7 (1), 27–34.

Glorioso, P.D., Flather, R.A., 1995. A barotropic model of the currents off SE South America. Journal of Geophysical Research 100, 13427–13440.

Glorioso, P.D., Simpson, J.H., 1994. Numerical modeling of the M2 tide on the northern Patagonian Shelf. Continental Shelf Research 14, 267–278.

Guerrero, R.A., Guerrero, A.R., 1997. Masas de agua en la plataforma continental. In: Boschi, E.E. (Ed.), El Mar Argentino y sus recursos pesqueros. In: TOMO 1: Antecedentes históricos de las exploraciones en el mar y las características ambientales. Instituto Nacional de Investigaciones y Desarrollo Pesquero (INIDEP), Mar del Plata, Argentina. 223 pp.

Kalnay, E., Kanamitsu, M., Kistler, R., Collins, W., Deaven, D., Gandin, L., Iredell, M., Sha, S., White, G., Woollen, J., Zhu, Y., Chelliah, M., Ebisuzaki, W., Higgins, W., Janowiak, J., Mo, K.C., Ropelewski, C., Wang, J., Leetmaa, A., Reynolds, R., Jenne, R., Joseph, D., 1996. The NCEP/NCAR 40-year reanalysis project. Bulletin of the American Meteorological Society 77 (3), 437–471.

Lucas, A.J., Guerrero, R.A., Mianzán, H.W., Acha, E.M., Lasta, C.A., 2005. Coastal oceanographic regimes of the Northern Argentine Continental Shelf (34–43 S). Estuarine, Coastal and Shelf Science 65 (3), 405–420.

Matano, R.P., Palma, E.D., 2008. On the upwelling of downwelling currents. Journal of Physical Oceanography 38 (11), 2482–2500.

Palma, E.D., Matano, R.P., Piola, A.R., 2004. A numerical study of the South Western Atlantic Shelf circulation: barotropic response to tidal and wind forcing. Journal of Geophysical Research 109, c08014. doi:10.1029/2004JC002315.

Palma, E.D., Matano, R.P., Piola, A.R., 2008. A numerical study of the Southwestern Atlantic Shelf circulation: stratified ocean response to local and offshore forcing. Journal of Geophysical Research 113, c11010. doi:10.1029/2007JC004720.

Pasquini, A.I., Depetris, P.J., 2007. Discharge trends and flow dynamics of South American rivers draining the southern Atlantic seaboard: an overview. Journal of Hydrology 333, 385–399.

Rivas, A.L., 2006. Quantitative estimation of the influence of surface thermal fronts over chlorophyll concentration at the Patagonian shelf. Journal of Marine Systems 63 (2006), 183–190. doi:10.1016/j.jmarsys.2006.07.002.

Rivas, A.L., Dogliotti, A.I., Gagliardini, D.A., 2006. Satellite-measured surface chlorophyll variability in the Patagonian shelf. Continental Shelf Research 26 (2006), 703–720. doi:10.1016/j.csr.2006.01.013.
Romero, S.I., Piola, A.R., Charo, M., Eiras Garcia, C.A., 2006. Chlorophyll-a variability off Patagonia based on SeaWiFS data. Journal of Geophysical Research 111, C05021. doi:10.1029/2005JC003244.
Sabatini, M.E., Martos, P., 2002. Mesozooplankton features in a frontal area off northern Patagonia (Argentina) during spring 1995 and 1998. Scientia Marina 66, 215–232.
Sabatini, M., Reta, R., Matano, R., 2004. Circulation and zooplankton biomass distribution over the southern Patagonian shelf during late summer. Continental Shelf Research 24, 1359–1373.
Sánchez, R.P., Alheit, P., Martos, P., Pájaro, M., 1998. The spawning and early life of *Engraulis anchoita* in the tidal fronts off Patagonia. ICES Annual Meeting, Caiscais, Portugal, 16–19 September. ICES C.M. 1998/R:01, 1 pp.
Saraceno, M., Provost, C., Piola, A.R., Bava, J., Gagliardini, D.A., 2004. Brazil Malvinas frontal system as seen from 9 years of AVHRR data. Journal of Geophysical Research 109, c05027. doi:10.1029/2003JC002127.
Saraceno, M., Provost, C., Piola, A.R., 2005. On the relationship between satellite retrieved surface temperature fronts and chlorophyll-a in the Western South Atlantic. Journal of Geophysical Research 110, c11016. doi:10.1029/2004JC002736.
Shimada, T., Sakaida, F., Kawamura, H., Okumura, T., 2005. Application of an edge detection method to satellite images for distinguishing sea surface temperature fronts near the Japanese coast. Remote Sensing of Environment 98, 21–34.
Ullman, D.S., Cornillon, P.C., 2000. Evaluation of front detection methods for satellite-derived SST data using in situ observations. Journal of Atmospheric and Oceanic Technology 17 (12), 1667–1675.
Ullman, D.S., Cornillon, P.C., 2001. Continental shelf surface thermal fronts in winter off the northeast US coast. Continental Shelf Research 21, 1139–1156.
Ullman, D.S., Cornillon, P.C., Shan, Z., 2007. On the characteristics of subtropical fronts in the North Atlantic. Journal of Geophysical Research 112, C01010. doi:10.1029/2006JC003601.